

Determining the Conformational Landscape of  $\sigma$  and  $\pi$  Coupling Using *para*-Phenylene and “Aviram–Ratner” BridgesDaniel E. Stasiw,<sup>†</sup> Jinyuan Zhang,<sup>†</sup> Guangbin Wang,<sup>†,||</sup> Ranjana Dangi,<sup>‡</sup> Benjamin W. Stein,<sup>‡</sup> David A. Shultz,<sup>\*,†</sup> Martin L. Kirk,<sup>\*,‡</sup> Lukasz Wojtas,<sup>§</sup> and Roger D. Sommer<sup>†</sup><sup>†</sup>Department of Chemistry, North Carolina State University, Raleigh, North Carolina 27695-8204, United States<sup>‡</sup>Department of Chemistry, The University of New Mexico, MSC03 2060, 1 University of New Mexico, Albuquerque, New Mexico 87131-0001, United States<sup>§</sup>Department of Chemistry, University of South Florida, 4202 East Fowler Avenue, CHE 205, Tampa, Florida 33620-5250, United States

## S Supporting Information

**ABSTRACT:** The torsional dependence of donor–bridge–acceptor (D–B–A) electronic coupling matrix elements ( $H_{DA}$ , determined from the magnetic exchange coupling,  $J$ ) involving a spin  $S_D = 1/2$  metal semiquinone (Zn–SQ) donor and a spin  $S_A = 1/2$  nitronyl nitroxide (NN) acceptor mediated by the  $\sigma/\pi$ -systems of *para*-phenylene and methyl-substituted *para*-phenylene bridges and by the  $\sigma$ -system of a bicyclo[2.2.2]octane (BCO) bridge are presented and discussed. The positions of methyl group(s) on the phenylene bridge allow for an experimentally determined evaluation of conformationally dependent ( $\pi$ ) and conformationally independent ( $\sigma$ ) contributions to the electronic and magnetic exchange couplings in these D–B–A biradicals at parity of D and A. The trend in the experimental magnetic exchange couplings are well described by CASSCF calculations. The torsional dependence of the pairwise exchange interactions are further illuminated in three-dimensional, “Ramachandran-type” plots that relate D–B and B–A torsions to both electronic and exchange couplings. Analysis of the magnetic data shows large variations in magnetic exchange ( $J \approx 1\text{--}175\text{ cm}^{-1}$ ) and electronic coupling ( $H_{DA} \approx 450\text{--}6000\text{ cm}^{-1}$ ) as a function of bridge conformation relative to the donor and acceptor. This has allowed for an experimental determination of both the  $\sigma$ - and  $\pi$ -orbital contributions to the exchange and electronic couplings.

The degree of  $\pi$ -orbital overlap in conjugated organic donor–bridge–acceptor (D–B–A) triads is modulated by torsional rotations about the D–B and B–A bonds. Although the  $\pi$ -system typically dominates electronic contributions to D–A coupling, torsional distortions effectively inhibit  $\pi$ -resonance delocalization and dramatically reduce the magnitude of the electronic coupling,  $H_{DA}$ , between donor and acceptor. This is important since the magnitude of  $H_{DA}$  is central to modulating intramolecular electron transfer rates,<sup>2</sup> the efficiency of electron transport in single-molecule electronic devices,<sup>3,4</sup> and OLED band-gaps.<sup>5</sup>

Transition metal complexes with persistent SQ–B–NN (SQ = semiquinone; B = bridge; NN = nitronyl nitroxide) biradical ligands offer a unique platform to experimentally evaluate the electronic origins of bridge-mediated electronic coupling at high resolution and at parity of D and A. Previously, we used a combination of magnetic susceptibility, multicomponent spectroscopy, and electronic structure calculations to elucidate electronic structure contributions to the magnetic exchange/electronic coupling in a variety of SQ–B–NN systems coupled by different bridge fragments.<sup>6–13</sup> More specifically, we have shown that a single D  $\rightarrow$  A charge transfer excited configuration dominantly contributes to the bridge-mediated  $\pi$ -superexchange interaction ( $J_{SQ-NN}$ ) that couples the  $S = 1/2$  SQ and  $S = 1/2$  NN radicals. Herein, we present the first experimentally determined three-dimensional (3D) plot of  $H_{DA}$  as a function of both donor–bridge and bridge–acceptor bond torsions in a “Ramachandran-type”<sup>14</sup> plot. Our analysis provides a detailed evaluation of  $\sigma$  vs  $\pi$  contributions to the electronic and magnetic coupling in D–B–A constructs, with  $\sigma$ -interactions being effectively independent of bridge type ( $sp^2$  vs  $sp^3$ ) at parity of D and A, and bridge length (i.e., D–A distance).

For the D–B–A triads discussed in this work, McConnell defines  $H_{DA}$  as the product of the electronic coupling matrix elements that describes the pairwise interaction within a given D–B–A system ( $H_{DB}$ ,  $H_{BA}$ ) and the energy gap between the localized donor and bridge states ( $\Delta_{DB}$ ) as shown in eq 1.<sup>15</sup>

$$H_{DA} = \frac{H_{DB}H_{BA}}{\Delta_{DB}} \quad (1)$$

Additionally, the  $H_{DB}$  and  $H_{BA}$  electronic coupling matrix elements contained in eq 1 each possess a torsional dependence described by eq 2, where  $i$  and  $j$  index two adjacent units of the D–B–A system and  $H_{ij}^0$  is the intrinsic electronic coupling matrix element at  $\cos(\phi) = 0$ , where the two entities are coplanar.<sup>16,17</sup>

$$H_{ij} = H_{ij}^0 \cos(\phi) \quad (2)$$

Received: May 11, 2015

Published: July 8, 2015

Wasielowski,<sup>16</sup> Harriman,<sup>17</sup> and Wenger<sup>18</sup> have shown independently that photoinduced electron transfer derived  $H_{DA}$  values follow a  $\cos(\varphi)$  dependence for each nearest neighbor interaction within the D–B–A system. There is an inherent connection between intramolecular electron transfer rates and the magnitude of the electron transport in single-molecule devices.<sup>3,4</sup> Since electron transfer and molecular electron transport are each related to a bridge-dependent off-diagonal coupling matrix element, it is important to understand the magnitude of  $H_{DA}$  in systems where the structural relationship between the bridge and connecting elements is well understood. Venkataraman<sup>19</sup> and Mayor<sup>20</sup> have shown a torsional ( $\cos^2 \varphi$ ) dependence on single molecule conductance using a series of torsionally modified biphenyls. These studies solely focused on  $\pi$ -system contributions to the transport behavior. However, Newton<sup>21</sup> has described a modified McConnell superexchange model<sup>15</sup> that accounts for both  $\pi$ - and  $\sigma$ -contributions to the electronic coupling matrix element. Under quantum interference conditions, or when  $\pi$ -systems of the molecule are orthogonal, Ratner has indicated that  $\sigma$ -pathways may be extremely important and effectively compete with torsionally compromised  $\pi$ -pathways for molecular conductance.<sup>22</sup> As such, direct experimental evaluation of  $\sigma$ - and  $\pi$ -contributions to electronic coupling as a function of molecular bond torsions will contribute to furthering our understanding of the magnitude of the  $\sigma$ -contribution when coupling via the  $\pi$ -system is compromised.

Using a valence bond configuration interaction (VBCI) model,<sup>11,23</sup> eq 3, we have determined the electronic coupling matrix element,  $H_{SQ-NN}$ , for D–A in the absence of a bridge. Here,  $J_{DA} \equiv J_{SQ-NN}$ ,  $H_{DA} \equiv H_{SQ-NN}$ , and  $U$  and  $K_0$  are the mean  $SQ \rightarrow NN$  charge transfer (CT) energy and the singlet–triplet splitting within the CT excited state, respectively. The magnetic exchange interaction,  $J_{DA}$ , and spectroscopic parameters  $U$  and  $K_0$  are all experimental observables that allow us to experimentally evaluate  $H_{DA}$  as a function of bridge type and bridge length.<sup>11</sup>

$$J_{DA} = \frac{H_{DA}^2 K_0}{U_2 - K_0^2} \quad (3)$$

For metal complexes of our D–B–A biradical ligands, configurational mixing of the  $SQ \rightarrow NN$  CT state into the ground state also results in an exchange splitting of the ground state to yield a singlet–triplet gap ( $= 2J_{DA}$ ), which is a fit parameter in the analysis of variable-temperature magnetic susceptibility data. Values of  $H_{DA}$  for a given **SQ-Bridge-NN** complex can then be determined conveniently from the ratio  $J_{SQ-B-NN}/J_{SQ-NN}$  ( $= H_{SQ-B-NN}^2/H_{SQ-NN}^2$ ) where **SQ-NN** is the “parent,” nonbridged biradical complex for which both  $J_{SQ-NN}$  and  $H_{SQ-NN}$  have been experimentally determined.<sup>6,9,11</sup>

The exchange interaction in these **SQ-Bridge-NN** systems can be mediated by both the  $\sigma$ - and  $\pi$ -orbitals of the bridge ( $J_{DA} = J_\sigma + J_\pi$ ) yielding pathway dependent contributions to the  $J$ -values. The  $\pi$ -pathway is expected to display a pairwise  $\cos\phi$  conformational dependence on the electronic coupling and  $\cos^2\phi$  conformational dependence magnetic exchange couplings as a function of the individual  $SQ$ -Ph and Ph-NN bond torsions. In marked contrast, electronic and magnetic exchange couplings mediated by the  $\sigma$ -pathway are less well understood but have been suggested to be a function of bridge type, contact symmetry, and D–B, B–B, and B–A bond torsions.<sup>24–26</sup> Complexes **1-Ph** and **1-PhMe<sub>4</sub>** were synthesized in order to evaluate the torsional dependence of the  $\sigma$ - and  $\pi$ -systems on the magnitude of  $J_{DA}$

(Figure 1, see Figure S1A for magnetic susceptibility plots and fit details) as described previously.<sup>6,9,11</sup> We also synthesized **1-**

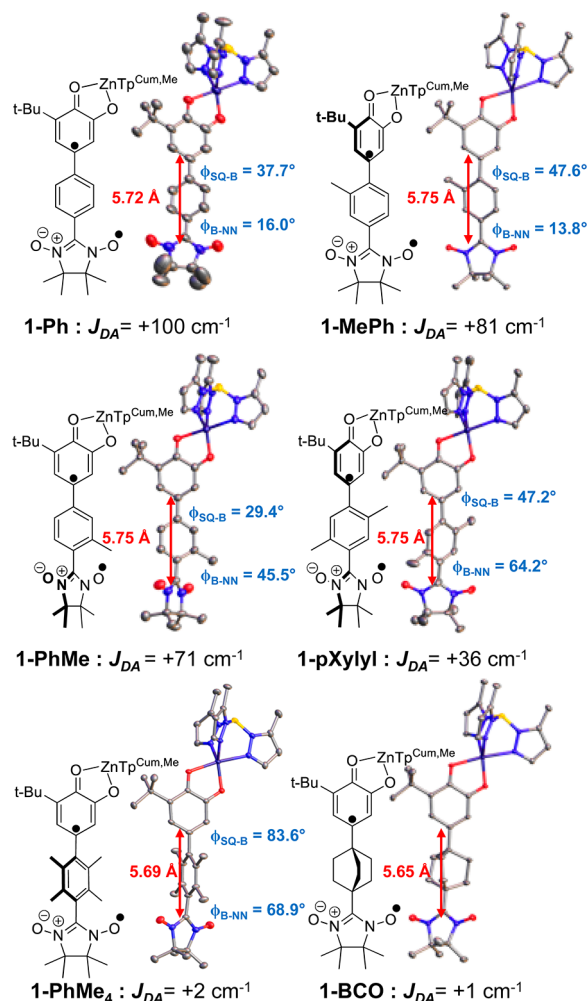


**Figure 1.** Bond-line drawings, thermal ellipsoid plots (hydrogen atoms and cumenyl groups omitted for clarity), donor and acceptor torsion angles, magnetic exchange coupling parameters ( $J_{SQ-NN}$ ), and donor–acceptor distances (Å) of complexes studied in this work. Donor–acceptor distances are listed for  $C_{ipso, SQ}-C_{ipso, NN}$ . The structure of **1-Ph** was reported previously.<sup>1</sup>

**BCO**, which possesses the “Aviram–Ratner” diode bridge bicyclo[2.2.2]octane, to evaluate  $J_\sigma$  and  $H_\sigma$  explicitly in the absence of any  $\pi$ -contributions to the exchange and electronic coupling (see Supporting Information for synthetic details). The variation in  $SQ-B$  and  $B-NN$  bond torsions are also given in Figure 1 along with thermal ellipsoid plots for **1-Ph**, **1-MePh**, **1-PhMe**, **1-pXylyl**, **1-PhMe<sub>4</sub>**, and **1-BCO** (BCO = bicyclo[2.2.2]octane; see Table S1 for crystallographic details). Torsion angles for the (substituted) phenyl complexes were determined using the mean planes of the  $SQ$  rings and bridge rings ( $\phi_{SQ-B}$ ), and the O–N–C–N–O atoms of  $NN$  and bridge rings ( $\phi_{B-NN}$ ).

Utilizing the crystallographically determined  $\phi_{SQ-B}$  and  $\phi_{B-NN}$  torsion angles (Figure 1), 3D plots have been constructed that relate both the electronic coupling and the magnetic exchange to donor–bridge and bridge–acceptor torsions in these **SQ-Bridge-NN** complexes (Figure 2). The experimental data is overlaid on top of a color-coded grid constructed from CASSCF calculated  $J$ -values for various **SQ-Bridge-NN**  $\phi_{SQ-B}$  and  $\phi_{B-NN}$  torsion angles. Least-squares fitting of the experimental data to

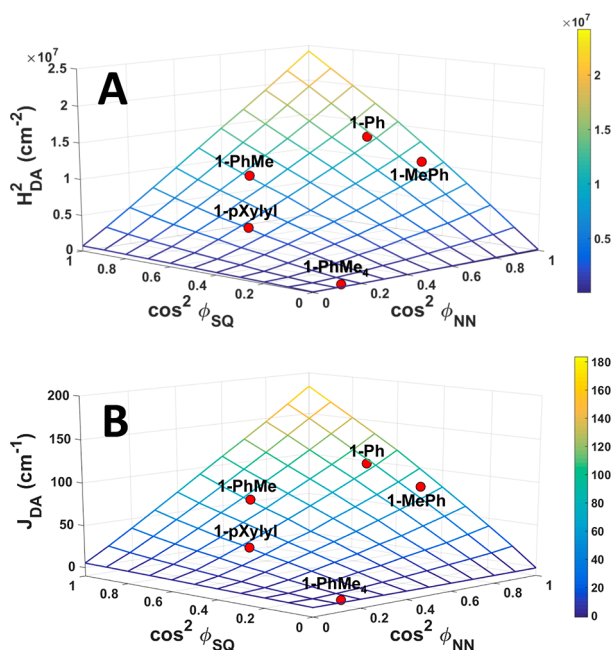


**Figure 2.** Electronic coupling (A) and exchange coupling (B) versus cosine-squared of the SQ-Ph torsion angle versus cosine-squared of the Ph-NN torsion angle for the *para*-phenylene bridged complexes. Data points for  $J$ -values were determined as best fit parameters to the variable-temperature magnetic susceptibility data (see Supporting Information). The 3D grid of  $J$ -values represents results from CASSCF calculations. Values for the electronic coupling and 3D grid (A) were calculated via eq 3.

the CASSCF surface function reveals an excellent correlation described by  $R^2 = 0.899$  for both the electronic- and exchange-coupling plots.

The **1-PhMe<sub>4</sub>** complex does not display perfectly perpendicular donor–bridge and bridge–acceptor fragments to allow for an exact evaluation of  $\sigma$ -only D–B–A communication. Thus, the  $\sigma$ -pathway has been explicitly evaluated using **1-BCO**, which possesses a saturated  $\sigma$ -only bridge entirely comprising  $sp^3$ -hybridized carbons, Figure 1. The exchange coupling parameter for **1-BCO** determined from a fit to the variable-temperature magnetic susceptibility data (see Figure S1B) is only  $J_{SQ-NN} = +1 \text{ cm}^{-1}$ , consistent with the value calculated from our CASSCF calculations. Thus, the predicted  $\sigma$ -superexchange through a *para*-phenylene ring perpendicular to both SQ and NN is equivalent ( $\sim 1.7 \text{ cm}^{-1}$ ), within the limitations of our susceptibility measurements, to the  $\sigma$ -superexchange mediated by a saturated BCO bridge.<sup>27</sup> Moreover, since all the carbon atoms of the phenylene ring are  $sp^2$  and those of the BCO bridge are  $sp^3$ , there is no measurable hybridization-dependent difference in the magnitude of the  $\sigma$ -contribution to the superexchange,<sup>28</sup> nor is there a measurable difference due to the fact that BCO comprises three  $-\text{CH}_2\text{CH}_2-$   $\sigma$ -pathways, while *para*-phenylene has just two pathways.

The conformational independence of  $J_\sigma$  for **1-BCO** can be understood with the aid of Figure 3. If we consider the view along the axis that contains both bridgehead carbons, the three  $C_{\text{bridgehead}}-C_{\text{ethano}}$   $\sigma$ -bonds transform as  $a_1$  and  $e$  in the local idealized  $C_{3v}$  symmetry of the bridgehead carbon. As per a hyperconjugative interaction, the degenerate  $e$ -symmetry set has the proper symmetry to mix with the  $p_\pi$  orbitals of the donor and acceptor. Orbital overlap of either the D or A spin containing  $p_\pi$ -orbitals with the first component of the  $e$ -set is shown in Figure 3,

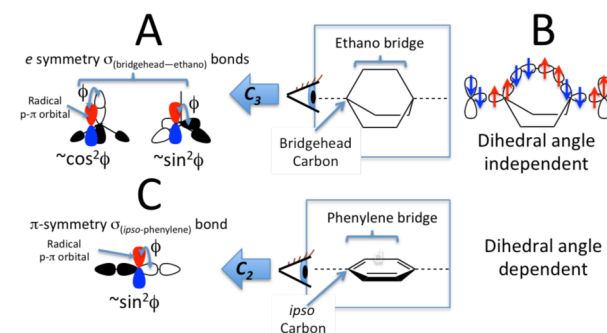


**Figure 3.** (A) Orbital argument for conformationally independent coupling of radical orbitals (red/blue) through the  $C_3$ -symmetric bicyclo[2.2.2]octane bridge orbitals (black/white). (B)  $\pi$ -Symmetry spin delocalization via bridgehead  $p_x$  and  $p_y$  orbitals and spin polarization via the  $p_z$  orbital (only one of the three bridge pathways have been depicted for clarity). (C) Orbital argument for conformationally-dependent  $\sigma$ -coupling through the  $C_2$ -symmetric phenylene bridge.

and this will display a  $\cos^2 \phi$  dependence. The second  $p_\pi$  component will display a  $\sin^2 \phi$  dependence on the orbital overlap. Since  $\cos^2 \phi + \sin^2 \phi = 1$  (a constant), coupling via hyperconjugation with the bicyclo[2.2.2]octane bridge is expected to be conformationally independent.<sup>27</sup> Additional support for the torsional independence of the  $\sigma$ -exchange coupling derives from methyl proton hyperfine computations on the ethyl radical ( $\text{CH}_3\text{CH}_2^\bullet$ ), which reveals average isotropic hyperfine coupling constants for the three methyl protons of 19.7 MHz (staggered geometry,  $\sim \cos^2 \phi$  in Figure 3A) and 19.6 MHz (eclipsed geometry,  $\sim \sin^2 \phi$  in Figure 3A).<sup>29</sup>

A second pathway for spin polarization, which is also independent of conformation, involves the  $\sigma$ -system and utilizes the  $a_1$  orbital of the bridgehead carbon. This is depicted in Figure 3B. Thus, regardless of the exchange mechanism (spin delocalization or spin polarization), coupling through the BCO bridge is expected to be conformationally independent.

As can be seen from Figures 1 and 2B, the values of  $J$  and  $H_{DA}$  for **1-PhMe<sub>4</sub>** are quite close to those of **1-BCO**. The small differences in these measured  $\sigma$ -mediated couplings most certainly originate from the differences in the  $sp^3$  and  $sp^2$  carbon centers of the respective bridges and the fact that there are two pathways for the  $sp^2$   $\sigma$ -bridge and three pathways for the  $sp^3$   $\sigma$ -bridge. Nevertheless, the magnitudes of the couplings suggest weak, conformationally independent  $\sigma$ -superexchange is operative in the phenylene series as well (favoring a spin polarization mechanism analogous to Figure 3B). Thus,  $\sigma$ -type magnetic exchange and electronic coupling appears to be bridge-carbon hybridization independent, suggesting a spin polarization mechanism for the  $\sigma$ -magnetic exchange in phenylene bridged systems that are orthogonal to D and A.

We have shown that D–B–A triads with nearest-neighbor torsional dependence of the exchange-/electronic coupling for *para*-phenylene-bridged D–B–A biradical complexes can be described by a 3D surface with torsionally independent  $H_{DB}$  and  $H_{BA}$  couplings. The data indicate that when the phenylene bridge is perpendicular to either D or A ( $\cos(\phi_{SQ-B}) = \cos(\phi_{B-NN}) = 0$ ) the  $\pi$ -contribution to electronic and magnetic couplings is zero, and a weak  $\sigma$ -only pathway dominates. The magnitude of the predicted electronic coupling at conformations with orthogonal D/A–B dihedral angles is determined by the magnitude of the exchange parameter measured for **1-BCO** ( $J_{SQ-NN} = +1 \text{ cm}^{-1}$ ).



Accordingly, the  $\pi$ -contribution to electronic coupling is  $\sim 13$  times greater than the  $\sigma$ -contribution for a planar SQ-Ph-NN system ( $H_{DA\pi}/H_{DA\sigma} \propto \sqrt{J_{\pi}/J_{\sigma}} = \sqrt{(180/1)}$ ). Our results include experimentally determined values of  $\sigma$ - and  $\pi$ -contributions to electronic coupling and a minimal dependence of  $\sigma$ -mediated electronic coupling on the carbon hybridization of the bridge.

This work also has implications for furthering our understanding of conductance in  $\pi$ -conjugated molecular transport junctions when individual components of the  $\pi$ -system become decoupled. Here, we anticipate that conductance ( $G$ ) mediated by a molecular  $\pi$ -junction will be  $\sim 180$  times greater ( $(G_{\pi}/G_{\sigma}) \approx (J_{\pi}/J_{\sigma}) = (180/1) = 180$ ) than that mediated by the corresponding  $\sigma$ -system, in general accordance with theory.<sup>22,30</sup> Full details of the spectroscopy and computational studies for the biradicals presented here will be reported in a future manuscript.

## ■ ASSOCIATED CONTENT

### ■ Supporting Information

Experimental and computational details. Synthetic- and X-ray crystallographic details, magnetic susceptibility data and fits, as well as absolute energies (in Hartrees) and the coordinates of the atoms in all the molecules whose geometries were optimized. The Supporting Information is available free of charge on the ACS Publications website at DOI: 10.1021/jacs.5b04629.

## ■ AUTHOR INFORMATION

### Corresponding Authors

\*shultz@ncsu.edu

\*mkirk@unm.edu

### Author Contributions

<sup>||</sup>CombiBlocks, San Diego, California 92126, United States.

### Notes

The authors declare no competing financial interest.

## ■ ACKNOWLEDGMENTS

D.A.S. thanks the National Science Foundation (CHE-1213269) for financial support. D.E.S. thanks the Department of Education, Graduate Assistance in Areas of National Need (GAANN) Program for a Fellowship (Nanoscale Electronic and Energy Materials; P200A090041 and P200A120021). M.L.K. acknowledges the National Science Foundation (NSF CHE-1301142) for financial assistance. B.W.S. acknowledges NSF Grant No. IIA-1301346. The single crystal diffraction data for **1-PhMe** and **1-pXyl** were collected at the USF X-ray Facility, Department of Chemistry, University of South Florida, Tampa.

## ■ REFERENCES

- (1) Shultz, D. A.; Vostrikova, K. E.; Bodnar, S. H.; Koo, H.-J.; Whangbo, M.-H.; Kirk, M. L.; Depperman, E. C.; Kampf, J. W. *J. Am. Chem. Soc.* **2003**, *125*, 1607.
- (2) Weiss, E. A.; Tauber, M. J.; Kelley, R. F.; Ahrens, M. J.; Ratner, M. A.; Wasielewski, M. R. *J. Am. Chem. Soc.* **2005**, *127*, 11842.
- (3) Ratner, M. *Nat. Nanotechnol.* **2013**, *8*, 378.
- (4) Nitzan, A. *J. Phys. Chem. A* **2001**, *105*, 2677.
- (5) Oberhumer, P. M.; Huang, Y.-S.; Massip, S.; James, D. T.; Tu, G.; Albert-Seifried, S.; Beljonne, D.; Cornil, J.; Kim, J.-S.; Huck, W. T. S.; Greenham, N. C.; Hodgkiss, J. M.; Friend, R. H. *J. Chem. Phys.* **2011**, *134*, 114901.
- (6) Kirk, M. L.; Shultz, D. A.; Stasiw, D. E.; Lewis, G. F.; Wang, G.; Brannen, C. L.; Sommer, R. D.; Boyle, P. D. *J. Am. Chem. Soc.* **2013**, *135*, 17144.
- (7) Kirk, M. L.; Shultz, D. A.; Stasiw, D. E.; Habel-Rodriguez, D.; Stein, B.; Boyle, P. D. *J. Am. Chem. Soc.* **2013**, *135*, 14713.
- (8) Kirk, M. L.; Shultz, D. A. *Coord. Chem. Rev.* **2013**, *257*, 218.
- (9) Kirk, M. L.; Shultz, D. A.; Depperman, E. C.; Habel-Rodriguez, D.; Schmidt, R. D. *J. Am. Chem. Soc.* **2012**, *134*, 7812.
- (10) Kirk, M. L.; Shultz, D. A.; Habel-Rodriguez, D.; Schmidt, R. D.; Sullivan, U. *J. Phys. Chem. B* **2010**, *114*, 14712.
- (11) Kirk, M. L.; Shultz, D. A.; Depperman, E. C.; Brannen, C. L. *J. Am. Chem. Soc.* **2007**, *129*, 1937.
- (12) Bin-Salamon, S.; Brewer, S. H.; Depperman, E. C.; Franzen, S.; Kampf, J. W.; Kirk, M. L.; Kumar, R. K.; Lappi, S.; Peariso, K.; Preuss, K. E.; Shultz, D. A. *Inorg. Chem.* **2006**, *45*, 4461.
- (13) Kirk, M. L.; Shultz, D. A.; Depperman, E. C. *Polyhedron* **2005**, *24*, 2880.
- (14) Issa, J. B.; Krogh-Jespersen, K.; Isied, S. S. *J. Phys. Chem. C* **2010**, *114*, 20809.
- (15) McConnell, H. M. *J. Chem. Phys.* **1961**, *35*, 508.
- (16) Davis, W. B.; Ratner, M. A.; Wasielewski, M. R. *J. Am. Chem. Soc.* **2001**, *123*, 7877.
- (17) Benniston, A. C.; Harriman, A.; Li, P.; Patel, P. V.; Sams, C. A. *Phys. Chem. Chem. Phys.* **2005**, *7*, 3677.
- (18) Hanss, D.; Wenger, O. S. *Eur. J. Inorg. Chem.* **2009**, *2009*, 3778.
- (19) Venkataraman, L.; Klare, J. E.; Nuckolls, C.; Hybertsen, M. S.; Steigerwald, M. L. *Nature* **2006**, *442*, 904.
- (20) Vonlanthen, D.; Mishchenko, A.; Elbing, M.; Neuburger, M.; Wandlowski, T.; Mayor, M. *Angew. Chem., Int. Ed.* **2009**, *48*, 8886.
- (21) Newton, M. D. *Int. J. Quantum Chem.* **2000**, *77*, 255.
- (22) Solomon, G. C.; Andrews, D. Q.; Van Duyne, R. R.; Ratner, M. A. *ChemPhysChem* **2009**, *10*, 257.
- (23) Tuzek, F.; Solomon, E. I. *Coord. Chem. Rev.* **2001**, *219*, 1075.
- (24) Hadt, R. G.; Gorelsky, S. I.; Solomon, E. I. *J. Am. Chem. Soc.* **2014**, *136*, 15034.
- (25) Ricks, A. B.; Solomon, G. C.; Colvin, M. T.; Scott, A. M.; Chen, K.; Ratner, M. A.; Wasielewski, M. R. *J. Am. Chem. Soc.* **2010**, *132*, 15427.
- (26) Su, T. A.; Li, H.; Steigerwald, M. L.; Venkataraman, L.; Nuckolls, C. *Nat. Chem.* **2015**, *7*, 215.
- (27) Beratan, D. N. *J. Am. Chem. Soc.* **1986**, *108*, 4321.
- (28) Goldsmith, R. H.; Vura-Weis, J.; Scott, A. M.; Borkar, S.; Sen, A.; Ratner, M. A.; Wasielewski, M. R. *J. Am. Chem. Soc.* **2008**, *130*, 7659.
- (29) Chipman, D. M. *J. Chem. Phys.* **1991**, *94*, 6632.
- (30) Solomon, G. C.; Bergfield, J. P.; Stafford, C. A.; Ratner, M. A. *Beilstein J. Nanotechnol.* **2011**, *2*, 862.